Limnol. Oceanogr., 49(1), 2004, 271–282

Empirical modeling of summer lake surface temperatures in southwest Greenland

Helen Kettle[1] *and Roy Thompson*
Department of Geology and Geophysics, The University of Edinburgh, Grant Institute, West Mains Road, Edinburgh EH9 3JW, UK

N. John Anderson[2]
Geological Survey of Denmark and Greenland (GEUS), Øster Voldgade 10, DK-1350 Copenhagen K, Denmark

David M. Livingstone
Water Resources Department, Swiss Federal Institute of Environmental Science and Technology (EAWAG), Überlandstrasse 133, CH-8600 Dübendorf, Switzerland

Abstract

This work presents a method to estimate mean daily lake surface water temperatures using only air temperature, theoretical clear-sky solar radiation, and lake size. Surface water temperatures were measured at a selection of lakes in southwest Greenland during the summers of 1998–2000. The lakes are small (surface area <150 ha) with maximum depths ranging from 3.5 to 47 m. An empirical model requiring only local air temperature and theoretical clear-sky solar radiation is developed to predict daily mean lake surface temperatures in summer for each lake. The model approximates the slow integrated response of water temperature to meteorological forcing by applying an exponential smoothing filter to air temperature. Exponential smoothing results in a 35% improvement in model fit compared with a model using unsmoothed air temperatures. The smoothed air temperatures and clear-sky solar radiation are linearly combined to estimate the daily mean lake surface temperatures. The smoothing parameters and the three linear coefficients of the model, obtained individually for each of 15 lakes, are found to relate to lake area and maximum depth, leading to the development of a general model. With this general model it is possible to predict the summer surface temperatures at any lake in this region where local air temperatures can be estimated. Cross-validation of the general model at each lake in turn indicated a 90% forecast skill and average standard error of prediction of 1.0°C. Examination of the daily prediction errors over time suggests a relation to strong wind events.

Water temperature plays a significant role in the functioning of lake ecosystems. It affects thermal stratification, the solubility of dissolved oxygen, the metabolism and respiration of lake fauna and flora, and the toxicity of pollutants (Stefan et al. 1998). The area around Søndre Strømfjord in southwest Greenland contains a considerable number of lakes, few of which have been studied systematically until now. The lakes are typically Arctic, in that they have a brief ice-free summer season. Because the chemical and biological status of any lake is strongly related to the development and evolution of the thermal stratification of the water column (Catalan 1988), the local climate during these ice-free months is crucial to the lake ecosystem.

The lakes, located between the Greenland ice cap to the east and the Davis Strait to the west, are in an area of considerable importance to global climate. This region is presently cooling (average decrease in annual temperature of 1.29°C from 1961–2001), presumably as a result of the current positive tendency of the North Atlantic Oscillation (Hanna and Cappelen 2003). In an attempt to develop predictive models from chironomids preserved in lake sediments to address Holocene climate variability, we measured lake surface temperature (LST) with miniature thermistors with integrated automatic dataloggers (cf. Livingstone et al. 1999). Microfossil environmental modeling requires a minimum of 40–50 lakes for calibration, but in this remote region, it is not feasible to deploy thermistors in every lake. An alternative approach is therefore required to estimate LST for use in these models.

Numerical process–based models of lake water temperature (e.g., Kraus and Turner 1967; Hondzo and Stefan 1993; Peeters et al. 2002) require detailed time series of meteorological data to drive them. Because such detailed and

[1] To whom correspondence should be addressed. Present address: Institute for Meteorology, The University of Edinburgh, James Clerk Maxwell Building, King's Buildings, Mayfield Road, Edinburgh EH9 3JZ, UK.

[2] Present address: Department of Geography, Loughborough University, Loughborough LE11 3TU, UK.

Acknowledgments

Fieldwork assistance was provided by Simon Patrick, Sherilyn Fritz, and Torben Lauridsen. Meteorological data from the five WMO stations were made available by the National Climate Data Center (NCDC), U.S. National Oceanic and Atmospheric Administration (NOAA).

Funding was provided by the European Union (contract EVKI-CT-1999-00032), the Danish Natural Science Research Council (SNF), and the Swiss Federal Office of Education and Science (contract 99.0394-2) within the framework of the European Union Environment and Climate project EMERGE (European mountain lake systems—regionalization, diagnostics, and socioeconomic evaluation). Fieldwork was undertaken with the financial assistance of the Geological Survey of Denmark and Greenland (GEUS) and the Commission for Scientific Research in Greenland.

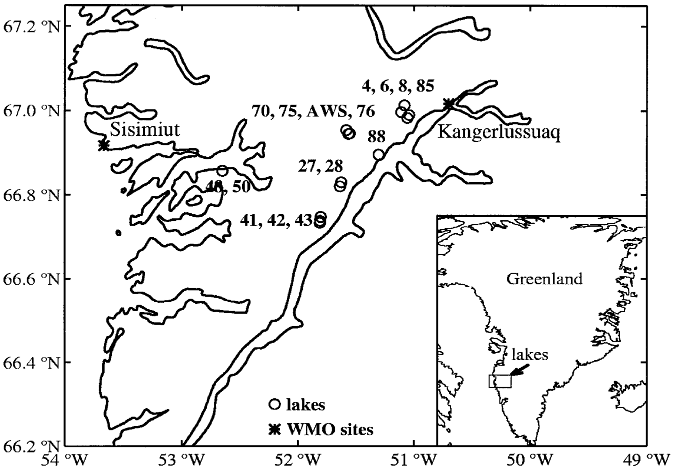

Fig. 1. Location of lakes, automatic weather station (AWS), and the closest World Meteorological Organization (WMO) observatories.

comprehensive data sets are not available for southwest Greenland, an empirical model is developed here to predict LST. Although the validity of any empirical model is limited by the dataset used in its construction, the empirical approach has pragmatic advantages for practical applications on a regional scale. These advantages lie in the limited amounts of input data required and in the comparative simplicity of application. Previous attempts to model LST empirically from air temperature alone have been quite successful on annual (Shuter et al. 1983), monthly (McCombie 1959), and daily (Livingstone and Lotter 1998; Livingstone et al. 1999) time scales. However, these studies relied on a direct linear relationship between LST and air temperature and did not attempt to incorporate either a time lag or smoothing into the models. This study attempts to demonstrate the importance of these two processes in the empirical modeling of LSTs in southwest Greenland, and a general model is developed to estimate LST requiring only the measured inputs of air temperature and lake size.

Methods

Sites and measurements—Southwest Greenland contains numerous lakes that show minimal anthropogenic effects (Anderson and Bennike 1997) and a great diversity of limnological variation in terms of mixing, acidity, and salinity (Anderson et al. 2001). As part of the development of a chironomid-based transfer function (Brodersen and Anderson 2002), temperatures have been monitored in >30 lakes in this region over the period 1998–2000, along and around an E–W transect from the ice sheet near Kangerlussuaq to the outer coast south of Sisimiut (Fig. 1). However, none of the lakes were monitored over the full period, so each lake was monitored over the summers of either 1998 and 1999 or 1999 and 2000. A number of the lakes in this area have enhanced conductivities (~2,000–4,000 μS cm^{-1}; Williams 1991; Anderson et al. 2001). The oligosaline lakes have closed basins and have evaporated steadily through the Holocene with resultant increases in salt concentrations (McGowan et al. 2003). The climate in this area is low Arctic continental, and much of the area is on the boundary between subpolar and true polar climates. The mean annual air temperature at Kangerlussuaq (Fig. 1) is −6°C, although summer daytime temperatures can exceed 15°C. In summer, the days are long, but solar elevation is relatively low, resulting in low mean air temperatures. At the coast, the annual temperature range is reduced, with less extreme winters but cooler summers, mainly because of increased clouds and fog. In winter, daily mean temperatures can fall to −40°C because of cold winter winds from the nearby ice cap. The westernmost lakes in the region are subjected to slightly more maritime meteorological conditions (e.g., coastal fog banks and increased precipitation), but their overall climatic setting is still continental because of the enclosed nature of the Labrador Sea. Annual precipitation is very low at the head of the fjord (~150 mm yr^{-1}) but substantially higher (300–>400 mm yr^{-1}) at the coast. The study lakes are ice-free for about 3 months of the year, from mid- to late June until late September or early October, depending on their location and altitude.

Littoral thermistors were deployed ~25–30 cm below the water surface in about 1–1.5 m water depth. In 1999, thermistors were also deployed on chains located in the deepest part of the lakes, as well as in the littoral. The surface thermistor on each chain was located about 10–15 cm from the lake surface. Temperatures were measured at 30-min intervals from mid-June (ice melt) to mid-September in 1998 and at hourly intervals in 1999. Additionally, an automatic weather station (AWS) measuring air temperature, wind velocity, and wind direction was installed in the middle of the transect between lakes 75 and 76 (Fig. 1), providing half-hourly data during summer 1999 and since summer 2000. Meteorological conditions were monitored at five World Meteorological Organization (WMO) observatories between Sioralik (65.02°N, 52.55°W) and Egedesminde (68.70°N, 52.85°W), with the two closest of these situated at Sisimiut in the west and Kangerlussuaq in the east (Fig. 1).

Although water temperature data were obtained from a large number of lakes in this region, not all were used in this work. LSTs at lakes very near to the ice sheet did not show any correlation with our estimated air temperatures for this region. This could be because of cold winds blowing from the glacier or because of melt water entering the lakes. Therefore, five lakes situated very near to the ice sheet were eliminated from the analyses. Two lakes very near the coast were also eliminated because of the occurrence of persistent fogs that alter local meteorological conditions, affecting our ability to interpolate air temperatures at these sites. Thus, the 15 lakes chosen are those for which a reasonable estimate of local air temperature can be made. These lakes vary in depth from 3.5 to 47 m and are situated over an altitude range of 160–550 m above sea level along a 90-km E–W transect. Details of their morphology and location are given in Table 1 and Fig. 1.

Estimating air temperature at each lake—Construction of a model for the surface temperature of a specific lake requires, at the very least, an estimate of the local air temperature at the lake. Although this region is not mountainous,

Table 1. Location and physical details of the 15 lakes used in this study. Conductivity is the mean of all available measurements (Anderson et al. 2001). Maximum depth is derived from bathymetric surveys using hand-held echosounders.

Lake No.	Altitude (m)	Area (ha)	Maximum depth (m)	Latitude (°N)	Longitude (°W)	Mean electrical conductivity (μS cm^{-1})
4	170	73.0	23.0	66.990	51.042	2,538
6	175	21.5	12.8	66.997	51.110	3,476
8	190	14.6	10.4	67.013	51.082	364
27	550	7.3	3.5	66.820	51.638	43
28	540	3.7	8.8	66.830	51.628	39
41	160	50.0	12.4	66.747	51.804	89
42	300	6.7	12.5	66.738	51.811	333
43	335	9.5	7.5	66.733	51.812	116
48	380	2.6	3.7	66.857	52.651	28
50	330	6.0	5.0	66.857	52.653	24
70	235	76.6	47.0	66.954	51.583	2,510
75	340	144.0	47.0	66.946	51.554	195
76	345	8.4	21.0	66.945	51.564	322
85	178	24.6	13.0	66.983	51.057	604
88	330	10.3	12.5	66.896	51.305	122

there are altitude differences that must be taken into account when interpolating air temperatures between the surrounding WMO stations. Hanna and Valdes (2001) suggest a lapse rate correction of -5°C km^{-1} for this region, which in the absence of further data, was applied to all sites. Following this, it became apparent that the air temperature recorded at the AWS was much higher than expected from spatial interpolation of the WMO station temperatures because of the unfortunate siting of the WMO stations. The four coastal WMO stations record lower summer air temperatures than those inland because of coastal fogs and the moderating effect of the ocean, whereas the one inland WMO station is close to the ice margin and records lower summer temperatures because of cool winds blowing out from the ice sheet.

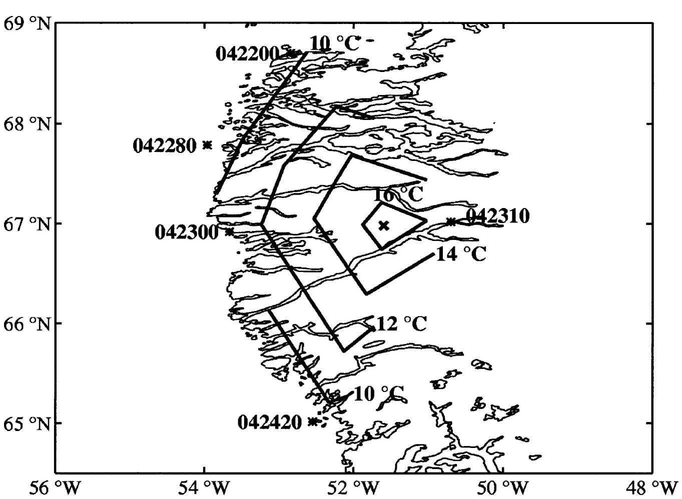

Fig. 2. Mean daily air temperature contours for 19 Aug 2000 showing large horizontal temperature gradients. This is a warm summer day identified in Fig. 3 as the second sharp peak of 2000. WMO stations are indicated by asterisks and their WMO identification number. The cross marks the site of the AWS.

The AWS is not strongly affected by either of these cooling phenomena, so air temperatures there tend to be higher than expected (Fig. 2). On a warm summer day, the difference between the temperature estimated by spatial interpolation of the WMO air temperature data and the actual daily mean air temperature at the AWS can be as much as 6°C. This changing horizontal air temperature gradient must be taken into account when estimating air temperatures in this region.

In 1999, the AWS operated only in summer, but from summer 2000 onward, it was in continuous operation. However, development of our LST model required daily mean air temperatures covering the same period as the water temperature measurements (summer 1998–2000). An air temperature transfer function was therefore constructed with data from the two closest WMO stations. The best procedure was found to be to construct a two-season model by dividing the year into ‘‘summer,’’ defined as that part of the year when the mean air temperature of the surrounding WMO stations was >0°C, and ‘‘winter,’’ in which mean air temperature was below 0°C. Figure 3 shows the fit of the two-season model for air temperatures at the AWS from 1999 to 2001. The transfer function output was thus used in combination with the AWS measurements to provide a continuous time series of air temperature at the AWS for the entire period for which LST measurements were available. This time series was used in conjunction with data from the five surrounding WMO stations, plus the lapse rate correction, to estimate the daily mean air temperature at each lake.

Estimating theoretical clear-sky solar radiation at each lake—In addition to air temperature, solar radiation is also an important determining factor of lake heat balances (e.g., Edinger et al. 1968), and therefore of LSTs. The solar radiation incident at any point on the earth's surface is essentially the theoretical clear-sky solar radiation at that point modified by cloud cover (e.g., Kasten and Czeplak 1980). Because information on cloud cover is not commonly avail-

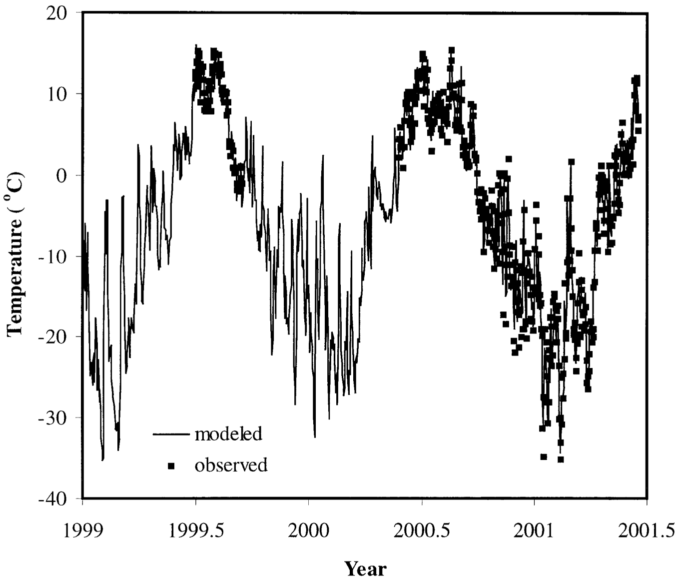

Fig. 3. Modeled and observed air temperatures at the AWS site.

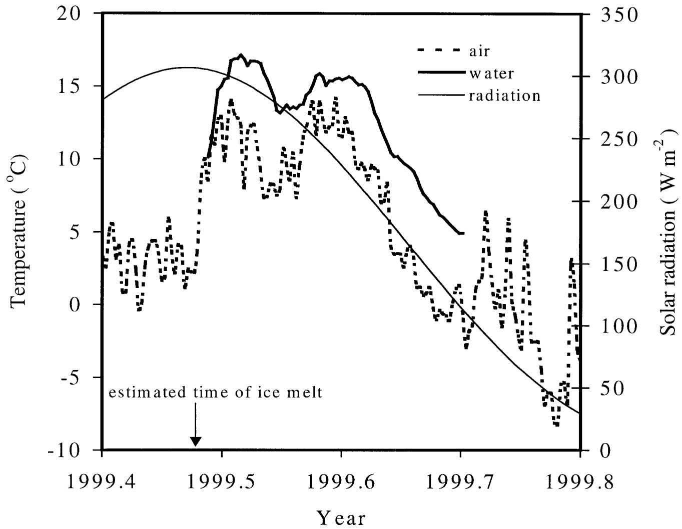

Fig. 4. Air temperature, surface water temperature, and theoretical clear-sky solar radiation at lake 42 in 1999. Note that the water temperature is well above air temperature but otherwise appears as a damped and delayed version of air temperature.

able, no attempt is usually made to incorporate solar radiation into empirical LST models. However, even without data on cloud cover, the theoretical clear-sky solar radiation alone can provide additional information that can be profitably incorporated into an empirical model of the kind described here. Hence, on the basis of the method outlined by Brock (1981), the theoretical clear-sky solar radiation incident on the surface of each of the lakes listed in Table 1 during the course of a year (neglecting local effects such as shading by local topography) was computed. The solar radiation incident at the top of the atmosphere was first computed by modifying the solar constant by a time-dependent factor to account for the effect of the ellipticity of the earth's orbit. Following Brock (1981), the separate effects of atmospheric attenuation on the direct and diffuse solar radiation were accounted for by applying the altitude-dependent exponential attenuation model of Hottel (1976) in conjunction with the empirical relationship between diffuse and direct solar radiation suggested by Liu and Jordan (1960). The degree to which clear-sky solar radiation is attenuated during its passage through the atmosphere is determined largely by the distance it travels through the atmosphere, which depends on the altitude of the lake and on the perceived solar elevation at the lake (Liu and Jordon 1960; Hottel 1976). The solar elevation, which also enters into the calculation of the component of the incident solar radiation perpendicular to the lake surface, is easily computed as a function of solar declination, latitude, and local time. The solar declination in this instance can be computed sufficiently accurately merely from the tilt of the earth's axis and the calendar date (e.g., Cooper 1969).

Summer surface water temperature model—The net heat flux between a lake and the atmosphere represents the net effect of five main heat exchange processes across the air/water interface (e.g., Sweers 1976). These are: the absorption of direct and diffuse short-wave solar radiation, the absorption of long-wave atmospheric radiation, the emission of long-wave radiation from the lake surface, the exchange of latent heat of evaporation and condensation, and the convective exchange of sensible heat (e.g., Edinger et al. 1968; Sweers 1976). These processes depend essentially on just four meteorological variables—air temperature, wind speed, relative humidity and cloud cover—and on one astronomical variable, the clear-sky solar radiation.

Air temperature is arguably the most important of the meteorological variables. It is causally involved in all heat exchange processes except the absorption of solar radiation and the emission of long-wave radiation from the lake surface (Edinger et al. 1968; Sweers 1976). In addition to this, it is often correlated to a certain extent with relative humidity and cloud cover, so that part of the climatic signal carried by these two variables is also present in air temperature. At any one time, the LST tends exponentially toward an equilibrium value that would theoretically result in zero net heat flux between lake and atmosphere (Edinger et al. 1968). This equilibrium temperature can be related quite strongly to ambient air temperature, but the influence on LST of the two radiation processes independent of air temperature, and of the other three meteorological variables, mean that this is not always the case (Dingman 1972).

Figure 4 shows an example of a comparison of the observed daily mean surface temperature of lake 42 with the corresponding estimated daily mean air temperature at the lake. The water temperature is typically 4–7°C warmer than the air temperature, a feature also noted in the European Alpine lakes (Livingstone et al. 1999). Otherwise, the water temperature is seen to follow the air temperature signal with a time delay and damping. Figure 4 also shows the calculated theoretical clear-sky solar radiation at lake 42. The estimated time of ice melt is seen to correspond fairly closely with the theoretical maximum clear-sky solar radiation. However, this is coincidental and is not true of all regions.

In the model described here, LSTs are assumed to be predominantly controlled by an exponentially smoothed version of the local air temperature. The adoption of this exponential smoothing filter is supported conceptually by the sensible heat exchange model of Rodhe (1952), cited by Bilello (1964), in which the change in LST with time is given by

$$\frac{dT_w}{dt} = k(T_a - T_w) \tag{1}$$

where T_w is the LST; t is time; T_a is air temperature; and k is a constant heat exchange coefficient with inverse dimension of time. Equation 1 can be integrated over time and formulated iteratively to give

$$T_{w,t} = (1 - e^{-k\Delta t})T_{a,t} + e^{-k\Delta t}T_{w,t-\Delta t} \tag{2}$$

(Rodhe 1952; Bilello 1964), where $T_{w,t}$ is the LST at time t, and Δt is a short time interval (in this application Δt is 1 d). Assuming that LST is related to air temperature by a smoothing function f, such that $T_{w,t} = f(T_{a,t})$, then

$$f(T_{a,t}) = \alpha T_{a,t} + (1 - \alpha)f(T_{a,t-\Delta t}) \tag{3}$$

where $\alpha = 1 - e^{-k\Delta t}$. Equation 3 is seen to be an exponential smoothing filter in which f is the smoothing function and α is the smoothing parameter in the interval [0, 1]. The smoothing parameter is thus a function of the heat exchange coefficient k and the time step Δt. When $\alpha = 1$, there is no smoothing, and as $\alpha \to 0$, the smoothing increases such that the current daily mean air temperature has much less affect on the water temperature. This smoothing function has the effect of reducing the variance of the air temperature data and incorporating a time delay.

In the sensible heat exchange model (Eq. 1) it is assumed that changes in water temperature are purely a function of air temperature. During long periods of cooling (e.g., during autumn and early winter up to the time of ice formation), this assumption appears to be empirically justified (Bilello 1964). In summer, however, when cooling because of the temperature difference between air and water at the lake surface is not the main factor that determines the thermal behavior of the epilimnion, Eq. 1 is unlikely to provide a sufficiently accurate description of the temporal variability of LST. This is confirmed for the specific case of the southwest Greenland lakes by the data in Fig. 4, which show that during summer, T_w consistently exceeds T_a. According to Eq. 1, this should result in a consistent decrease in T_w with time, which is clearly not the case. In summer, the net effect of the heat exchange processes mentioned above is to raise the equilibrium surface temperature of the southwest Greenland lakes above the ambient air temperature. To account for this, at least partially, in our model we include as a further variable the theoretical clear-sky solar radiation.

Multiple linear regression of our data shows that the LST can be modeled satisfactorily as a linear combination of exponentially smoothed air temperature and the theoretical clear-sky radiation S such that

$$T_w = a + bf(T_a) + cS \tag{4}$$

where a, b, and c are constants, and f is the exponential smoothing function. Because the theoretical clear-sky solar radiation S contains no information about cloud cover or any other meteorological processes that affect the LST on a daily or interannual basis, it can be viewed simply as an annual cycle. The five heat exchange processes mentioned above are represented in our four-parameter model by the intercept a, the scaling of the smoothed (f) air temperature b, and the cyclic term cS. The relative importance of these terms varies on an annual time scale such that the difference between the water temperature and the smoothed air temperature is large at the beginning of summer, becoming smaller in autumn as the solar radiation decreases. We restrict the model (Eq. 4) to water temperatures above 4°C because of the reversal in the density–temperature relationship that occurs at this temperature. This reversal means that the coupling between LST and air temperature is weaker for LSTs <4°C than for those >4°C. Additionally, the model is not applicable during the period immediately after ice melt, when the LST undergoes a sudden rapid rise toward the equilibrium temperature. The model can be identified as an empirical heat exchange model with a seasonal radiation component. The four model parameters are obtained by fitting predictions to LST measurements.

Results

Individual lake model—For each lake, an iterative process was used to find the smoothing parameter and linear coefficients in Eq. 4 that gave the best fit to the data in terms of mean absolute error. The results of a model fitted for one individual lake are shown in Fig. 5. This model fits well with $R^2 = 0.86$, although it slightly underestimates the summer peaks. The observed data appear more smoothed in 1999 than in 1998, which is probably indicative of a change in the mean depth of the epilimnion between the two years. The smoothing parameter is calculated with data from both years, leading to slight oversmoothing in 1998.

The other 14 lakes show similarly good fits (Table 2) with no obvious problems. The individual lake models can be used to hindcast and forecast summer water temperatures. However, in order to reconstruct water temperatures at lakes *without* thermistor data, it is necessary to develop a general model. The parameters found for each lake individually (as shown in Table 2) appear to be fairly consistent, with no dramatic leaps over several orders of magnitude that can be encountered when linear models overfit specific datasets. The intercept term, a, is a little unusual (negative) for lake 48, and the air temperature sensitivity is rather high (>1) for lake 50. Otherwise, the consistency is very encouraging, indicating that no gross overfitting has taken place. Similarly, the R^2 values all lie above 0.74. Because the R^2 values are all calculated with an annual cycle removed (i.e., they are based on anomaly data), they again point to very satisfactory models and suggest that a more general model could be developed.

To demonstrate the advantage of damping and time-lagging the air temperature, a second set of models was developed that used unsmoothed air temperatures. Figure 6 plots the daily output from all 15 individual lake models, with and without smoothing, against the observed data. The mean R^2 value for the simple linear model is 0.80 compared with 0.87

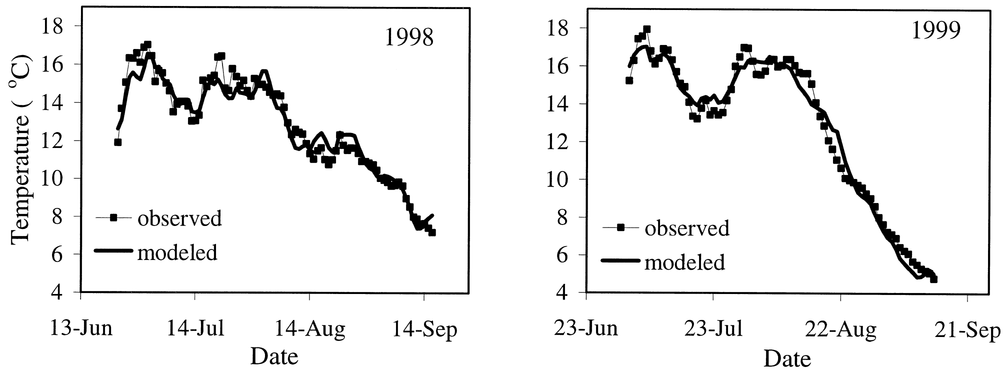

Fig. 5. Observed and modeled water temperatures from the individual lake model for lake 41 in 1998–1999.

for the smoothed linear model, and this, along with Fig. 6, clearly demonstrates the improvements in fit achieved by smoothing the air temperature. The mean absolute fit errors of the simple linear model and the linear model with smoothing are 0.94°C and 0.61°C, respectively. Thus, smoothing the air temperature results in a 35% decrease in error.

General model—Here, the overall aim is to predict daily mean summer surface water temperatures for any lake in this region of southwest Greenland where local air temperature can be estimated. To achieve a useful model, it is necessary to discover relationships between the model parameters (α, a, b, and c of Eq. 4) and the physical features of each lake. Most of the water temperature data were collected in 1999. To avoid bias in the parameter relations toward the mean meteorological conditions prevailing in 1999, the general model equations were also derived by weighted regression, with equal influence given to each year by increasing the weighting on data from 1998 and 2000.

The model parameters will be largely determined by the thermal stratification of the water column and, particularly, by the depth of the epilimnion (the mixing depth) because this determines the volume of water responding to changes in air temperature. However, we have no means of determining the mixing depth. Instead, stepwise multiple regression was performed to search for relationships between each of the parameters and the likely physical controls of maximum lake depth (D), lake surface area (A), and salinity (expressed in terms of conductivity). The smoothing parameter α was first transformed to $\tau = 1/\alpha$, the average age (in days) of the smoothed data (because $\alpha \leq 1$ by definition, $\tau \geq 1$ regardless of the size of the lake). The following relationship between τ (days), A (ha), and D (m) was then found.

$$\tau = 1 + 1.234 \ln D + 0.035A \tag{5}$$

Thus, Eq. 5 can be used to find the amount of smoothing needed at each lake on the basis of its maximum depth and surface area. This estimates the α values shown in Table 2 with $R^2 = 0.82$ and gives the mean absolute error in α as 0.035. The fit is shown in Fig. 7a.

Linear regression on the physical variables listed above was also used to find the three linear coefficients of the general model, such that

$$\mathrm{a} = -1.86 + 1.672 \ln D \quad (R^2 = 0.64;\ \mathrm{MAE} = 0.77°\mathrm{C}) \tag{6}$$

Table 2. Model parameters and R^2 values for each lake.

Lake No.	Smoothing parameter, α (°C^{-1})	Intercept, a (°C)	Air temperature coefficient, b	Solar radiation coefficient, c (°C m^2 W^{-1})	R^2
4	0.12	2.39	0.79	0.014	0.79
6	0.29	2.53	0.68	0.019	0.85
8	0.23	2.48	0.86	0.013	0.74
27	0.37	1.16	0.81	0.018	0.85
28	0.33	3.60	0.81	0.006	0.85
41	0.23	2.64	0.77	0.016	0.86
42	0.22	2.99	0.67	0.019	0.94
43	0.34	0.80	0.77	0.025	0.92
48	0.30	−0.26	0.94	0.025	0.84
50	0.31	0.21	1.03	0.019	0.91
70	0.13	5.39	0.64	0.003	0.91
75	0.09	4.79	0.53	0.004	0.98
76	0.17	2.43	0.63	0.018	0.84
85	0.13	0.34	0.98	0.017	0.85
88	0.23	2.97	0.75	0.013	0.90

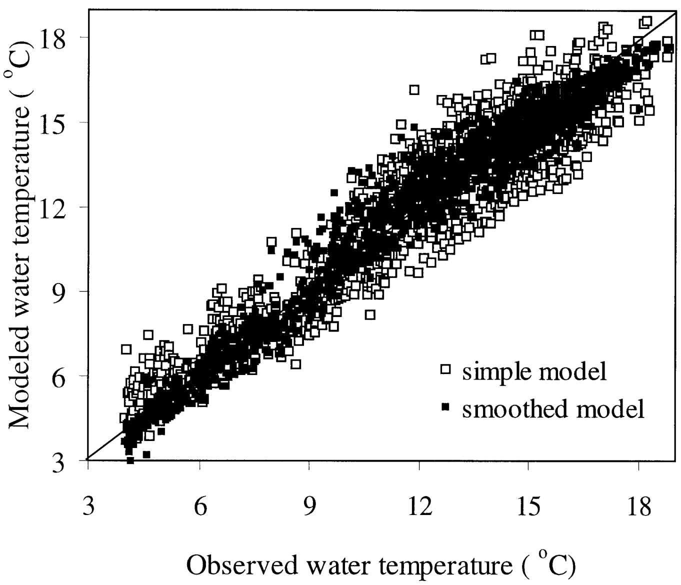

Fig. 6. Comparison of the fit of the simple linear models with the fit of the smoothed linear model for all lakes. The diagonal line indicates a perfect fit.

$$b = 1.087 - 0.125 \ln D$$
$$(R^2 = 0.50;\ \mathrm{MAE} = 0.08) \qquad (7)$$
$$c = 2.08 \times 10^{-2} - 3.44 \times 10^{-4} D$$
$$(R^2 = 0.51;\ \mathrm{MAE} = 0.003°\mathrm{C\ m^2\ W^{-1}}) \qquad (8)$$

Unlike the smoothing parameter, the linear coefficients were not found to be significantly dependent on lake area but largely controlled by the maximum depth D (m), as shown in Fig. 7b–d. Equations 5–8 thus provide a general model which, given lake surface area and maximum depth, can be driven by daily mean air temperatures (calculated by the interpolation method outlined earlier) and by theoretical clear-sky solar radiation to generate daily mean lake surface temperatures.

Model validation—To check the parsimony and predictive capabilities of the general model, Eqs. 5–8 were cross-validated by omitting each lake in turn and carrying out the full modeling procedure on the remaining 14 lakes to derive a new set of equations (Eqs. 5–8). LSTs at the verification lake were then predicted with the new general model (i.e., LSTs were modeled as if no data from the verification lake was available). Then, the modeled and observed water temperatures were compared, and model performance was assessed by four commonly employed criteria: (i) bias, which is simply the mean error of prediction (where the prediction error is given by subtracting the observed from the modeled data); (ii) the root mean square error (RMSE); (iii) the mean absolute error (MAE); and (iv) the forecast skill of Lorenz (1956) given by

$$\mathrm{skill} = 100\% \times \left[1 - \frac{\sum (x_i - \hat{x}_i)^2}{\sum (x_i - \bar{x}_c)^2}\right] \qquad (9)$$

where x_i and $\hat{x}_i$ are the actual and estimated water tempera-

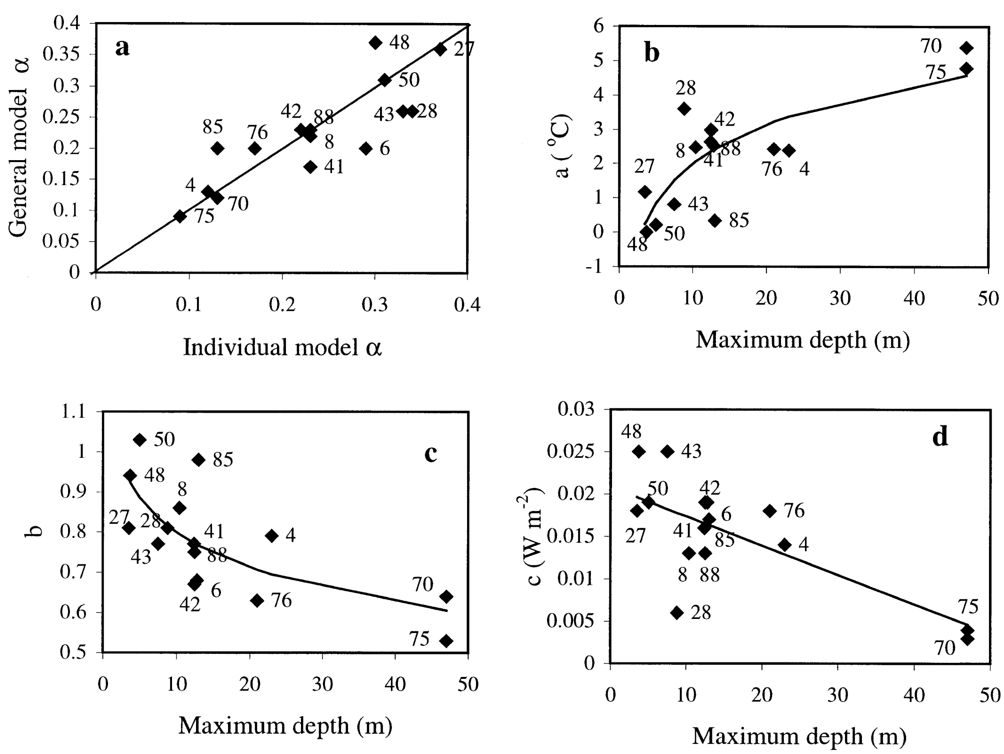

Fig. 7. The relationships for the general model parameters. (a) The fit of Eq. 6 for the smoothing parameter and (b–d) the relationships between the linear coefficients and maximum depth, in which the lines represent Eqs. 6–8. Labels indicate lake number.

Table 3. Model cross-validation prediction statistics for two different weighting methods. Bias, mean error of prediction; RMSE, root mean square error; MAE, mean absolute error; Skill, forecast skill of Lorenz (1956).

Weighting method	Bias (°C) All years	1998	1999	2000	RMSE (°C)	MAE (°C)	Skill (%)
None	−0.01	−0.47	−0.04	0.21	1.04	0.85	91
By year	0.05	−0.31	0.05	0.12	1.04	0.85	90

tures at the verification lake and $\bar{x}_c$ is the mean of the actual water temperatures at the calibration lakes. The closer the skill is to 100%, the better the prediction. Each of these criteria yields specific information about the model, and the employment of all three allows a comprehensive assessment of the model's predictive capabilities.

The cross-validation procedure was performed with and without the weighting previously described. Table 3 shows how the error statistics change according to the weighting strategy employed. With respect to RMSE, MAE, and forecast skill, the weighting method was found to have no significant influence on the outcome of the cross-validation. However, Table 3 clearly shows the reduction in bias for 1998 and 2000 achieved by employing the yearly weighting method, which allowed more accurate predictions in these years despite the overall increase in bias. Plots of prediction error against time (Fig. 8) indicate a definite time structure in the errors. In 1998, the water temperatures are generally underestimated, but in 2000, they are generally overestimated. In addition, in 1999, three episodes of overestimation followed by underestimation, each cycle lasting around 2 weeks, produced a triple-peaked pattern (Fig. 8). We suggest that these short-term cycles occur when the depth of the epilimnion deviates from its long-term mean. Thus, during a spell of hot, windless days, the epilimnion is thin and LSTs are higher than expected (i.e., the errors in Fig. 8 are negative), whereas on windy days, cooler water from the upper metalimnion is mixed upward, resulting in lower LSTs than expected. The results here suggest that each lake is affected by wind events to a different degree. In particular, the two lakes near the coast (lakes 48 and 50) appear to be less

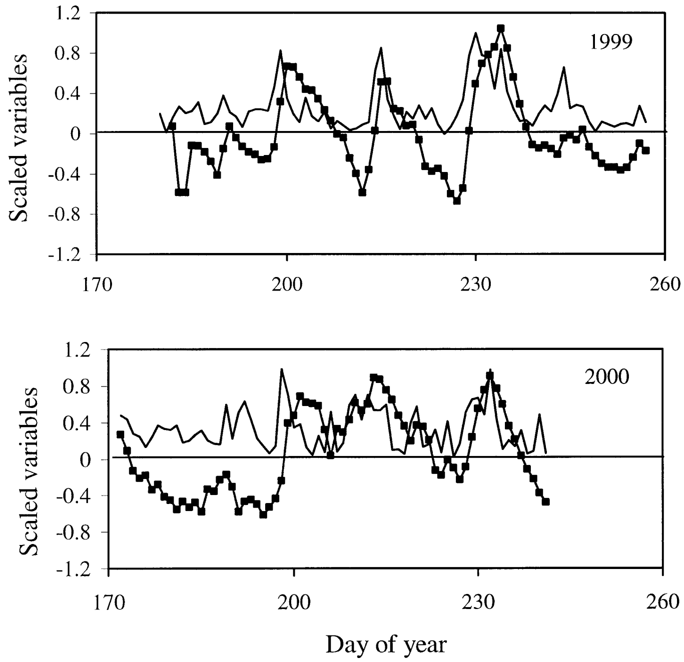

Fig. 9. Comparison of mean daily wind speed (solid line) and mean daily prediction errors (line with squares) at all lakes. To enable direct comparison, wind measurements are transformed to lie between 0 and 1, and prediction errors are transformed to a maximum amplitude of 1. In 1999, there is a clear correlation between these two variables.

affected than the others. The daily residuals averaged across all the lakes are compared with the wind speed measured at the AWS in 1999 and 2000. Figure 9 shows scaled versions of these variables to facilitate comparison. In 1999, it is clear that the three main wind events correspond, after a time delay, with the three peaks in the prediction error. The pattern is not as clear in 2000, perhaps because the wind events are less well defined. However, the effect of wind events on epilimnion temperatures is dependent on temperatures in the metalimnion and hypolimnion, implying that knowledge of the daily temperature profile would be necessary to incorporate the effects of wind mixing into the model. This would

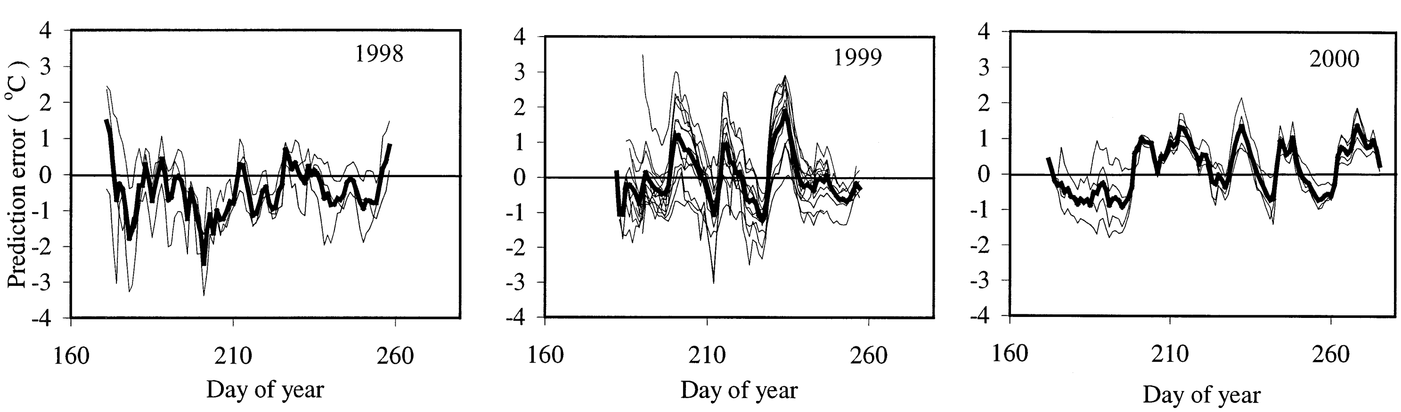

Fig. 8. Time structure in prediction errors. Thin lines indicate the prediction errors at each lake, thick lines indicate the daily mean of these errors.

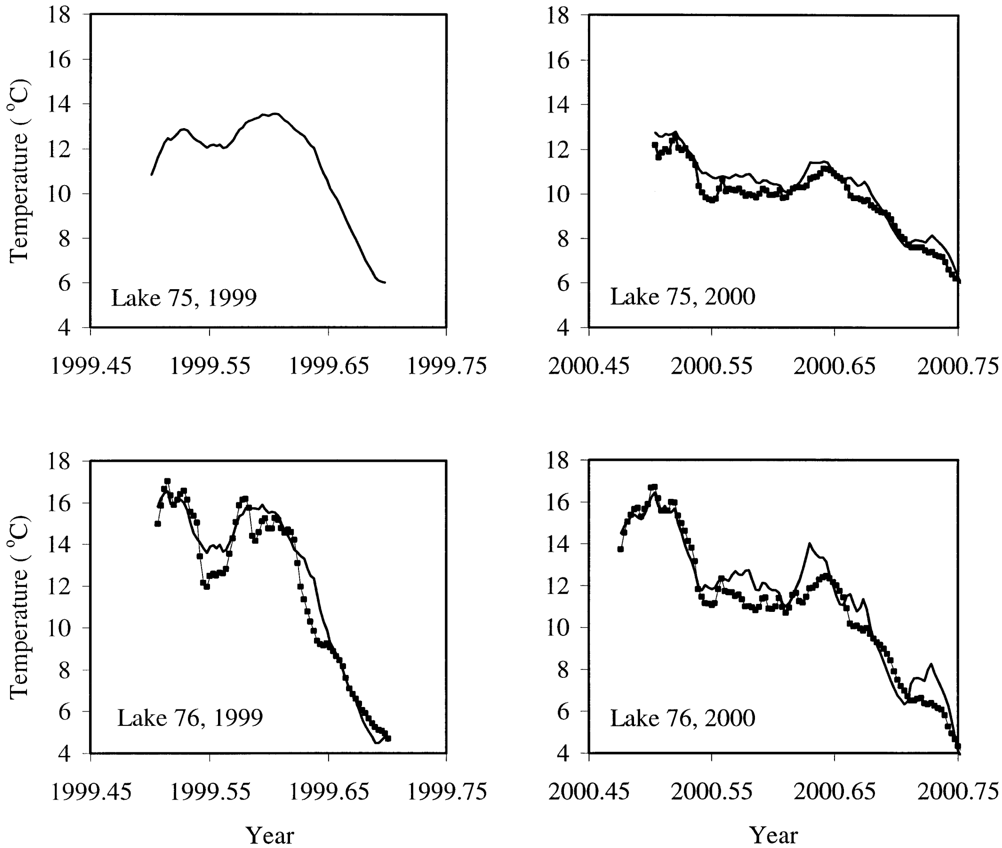

Fig. 10. Validation of the general model at lakes 75 and 76. The big difference in both depth and area between these two lakes results in large differences in their surface temperatures, which are reproduced well by the model. Observed data are represented by squares, modeled data by lines. Note that no water temperature observations are available for lake 75 in 1999.

require a deterministic water temperature model such as that described in Hondzo and Stefan (1993). For these reasons, and because wind speed is not as spatially coherent as air temperature and is therefore not a good empirical predictor over large regions, wind speed has not been included in this model.

Another way to test the general model is to compare surface temperature predictions for lakes of very different sizes. Lakes 75 and 76 have areas of 144 ha and 8.4 ha and maximum depths of 47 m and 21 m, respectively. These two lakes are situated a few meters either side of the AWS. Therefore, because our estimated air temperatures at these lakes should be correct and other meteorological effects identical, the differences in their surface temperatures must be a result predominantly of differences in their morphometry. The difference in mean temperature caused by their difference in size is seen easily in Fig. 10, in which the smaller lake 76 can be seen to have a much higher surface temperature than the larger lake 75. The substantial differences in temperature (~4.5°C at the summer peak) are predicted well by the model.

Discussion

Remarkably little is known about the thousands of lakes in southwest Greenland. This lack of baseline data makes it extremely difficult to predict the possible effects of future climate change in the Arctic on these lakes. Unlike the rest of the Arctic, southwest Greenland has cooled over the last 40 yr (Hanna and Cappelen 2003). The likely response of these lakes to this cooling or to a possible future regional warming is difficult to assess because little is known about their thermal structure. The monitored and modeled data generated for some of the lakes in southwest Greenland provide a valuable baseline dataset to use in numerical models that can evaluate the effect of possible future climate change on these lakes. It remains to be determined whether the cooling trend will continue and to what extent the resulting lower temperatures will be reflected in altered mixing regimes and lake surface temperatures. A simple data-based model such as that developed here will have parameters that are particular to the environmental conditions prevailing at the time of data collection; therefore, it is unwise to presume that this model could be used to predict or retrodict LSTs outside of the model-building time period. This is particularly true for this region because changes in the proximity of the ice sheet could dramatically affect LSTs.

The general empirical model developed here is consistent with the physical principles governing LSTs. The volume of water responding to external forcing is determined by the mixing depth (i.e., the depth of the epilimnion). However, because the mixing depth of each lake is not known, the morphometric variables, surface area, A, and maximum depth D are used to predict the model parameters under the assumption that the mixing depth is related to lake size and, hence, will be implicitly included in the empirical equations. According to Straskraba (1980), the mixing depth of freshwater lakes has an upper limit of 20–25 m, which might explain the presence of the logarithmic function of D in three of the parameter regression equations. As shown in Fig. 7, once $D \geq 15$ m, $\ln D$ increases by progressively smaller amounts, so that an upper limit on the mixing depth is implicitly included.

The smoothing parameter, α, describes the rate of response of the water temperature to changes in air temperature. Physically, this rate of response is controlled predominantly by the mixing depth. The reciprocal of the smoothing parameter, τ, which is a measure of the time over which the air temperature is smoothed, is directly proportional to A and to $\ln D$ (Eq. 5). Thus, large lakes are predicted to react more slowly to changes in air temperature (i.e., the response is averaged over a longer time period) than smaller lakes. This is in agreement with empirical relationships already determined relating mixing depth to wind fetch (e.g., Arai 1981; Shuter et al. 1983; Fee et al. 1996), which imply that larger lakes generally have a greater mixing depth. The three linear coefficients of our model (a, b, and c) will interact with each other to some extent, so it is difficult to draw physical conclusions from their relationships with A and D. However, both the intercept, a, and the air temperature coefficient, b, are found to be functions of $\ln D$ (Eqs. 6, 7), which might imply that they are dependent on mixing depth. It is possible that the intercept (a) is a function of the heat energy stored within the lake, and therefore represents a ''base level temperature.'' The air temperature coefficient (b) controls the sensitivity of the LST to air temperature. Thus, Eqs. 6 and 7 might imply that deep lakes have a higher base level temperature that is less sensitive to changes in air temperature, as opposed to shallower lakes, which have a low base level temperature but much larger fluctuations in LST. This hypothesis is supported to some extent because the study lake with the smallest surface area (lake 48) has a negative value for the intercept (a) and a high value for the air temperature coefficient (b = 0.94).

Because the mixing depth of a given lake is determined by temporally variable local meteorological driving forces and lake size, the parameter relationships identified in this study are presumably to a large extent expressions of regional climate and likely to be specific to southwest Greenland. That such relationships are at all apparent implies a large degree of regional coherence in the relevant meteorological driving forces across the region. The existence of a high degree of regional coherence in air temperature is apparent from the good correspondence between modeled and observed air temperatures illustrated in Fig. 3; such modeling would not be possible if the air temperatures measured at the WMO stations were not highly correlated. With regard to solar radiation, at least during early summer, local modulation of the clear-sky solar radiation by cloud cover is very low because many days are cloudless. Additionally, the lakes are located in a rolling landscape, so the great majority are unaffected by local shadowing from cirque walls, which can considerably lower LSTs (Livingstone et al. 1999). However, local effects such as turbidity and water color might be important. Secchi depths in this area range from <2 m to >15 m in lake 75, the clearest of the lakes sampled to date. Dissolved organic carbon concentrations are high in the closed basin lakes (>40 mg L^{-1}), but these lakes are colorless. Because there are strong climate gradients over this small region, the date of ice melt could have a strong influence on summer LSTs (Anderson and Brodersen 2001). Estimating LST in years when the date of ice melt differs greatly from the mean over 1998–2000 could necessitate recalculation of the model parameters.

Because LST predictions from the general model are highly dependent on the accuracy of the estimated air temperature, a more exact quantification of altitudinal air temperature lapse rates in the region would reduce one source of error. The typical environmental lapse rate globally is $-6.5°C\ km^{-1}$. In Greenland, values of $-5°C\ km^{-1}$ (Hanna and Valdes 2001) and $-7°C\ km^{-1}$ (Thompson and Pollard 1997) have been estimated. The value of $-5°C\ km^{-1}$ used in this study might not be accurate, but the bias errors in the prediction of LST at each lake were not correlated with altitude, implying that the lapse rate is not a significant source of error. The main source of error in this region appears to be wind events. Future empirical modeling studies could aim to include wind data in the relevant equations, but these would then have to involve nonlinear terms and require more measured input data.

Numerical process–based lake water temperature models use classical partial differential equations to describe heat exchange across the air–water interface and heat transport within the water column. However, such models are never entirely deterministic because many empirical relationships and empirically determined constants are incorporated into them. Such empirical relationships could be specific to the region in which they were determined, introducing errors into simulations conducted in other regions. In addition to these parameter errors, errors are also incurred by the discretization of continuous processes (e.g., numerical diffusion). The numerical simulation models used by Fang and Stefan (1996) and Stefan et al. (1998) require high-resolution weather data such as air temperature, dew point temperature, wind speed, solar radiation, total cloud cover, and precipitation. However, despite the detailed input data, the standard errors of prediction for the simulated water temperatures of the North American lakes used in these two studies were approximately 1.3°C and 1.4°C. Thus, the results obtained from our simple empirical model with a cross-validation standard error of only 1°C and only one measured meteorological input variable (air temperature) compare very favorably.

Although automatic dataloggers represent a relatively cost-effective method of measuring LST, it is still prohibitively expensive to deploy them in the numbers that would be required to develop a calibration dataset of the type needed for paleolimnological studies (Brodersen and Anderson 2002). A commonly employed alternative, that of spot samples taken simultaneously with water chemistry, by sediment sample collection, or by both methods is essentially meaningless given the inherent variability of LST over days and weeks (Hann et al. 1992). Given this problem, some studies have used lapse rate–corrected air temperatures instead of water temperatures (e.g., Lotter et al. 1997). Although clearly superior to spot samples, given the complex relationship between air and water temperatures, air temperatures might not reflect the ambient water temperature sufficiently well. The model developed here represents an alternative approach. Given the robustness of the model, it permits the estimation of LST for a whole suite of lakes within a given region, with good error statistics. Unfortunately, at the extremes of the area near the coast or ice sheet, the model cannot be applied because of the large uncertainties in air temperature estimations. However, the modeling approach detailed here could also be useful in other similarly remote regions with large numbers of lakes, such as northern Finland, Siberia, and northern Canada.

In summary, a general model for daily summer surface temperatures of lakes in southwest Greenland has been developed and validated. The only measured data required for this model are local daily mean air temperatures and lake size. Despite the small amount of input data required, the cross-validation errors from this model compare favorably to those produced from complex process-based models requiring large amounts of accurate high-resolution data.

Discrepancies between the modeled and observed water temperatures might result from inaccurate estimation of local air temperature, or from meteorological conditions that result in significant changes to the thermal stratification of the lake. In particular, strong wind events cause cold water to be mixed upward, creating cooler surface water temperatures, and conversely, calm warm periods allow strong stratification, creating warmer surface water temperatures.

The four model parameters are found to relate (in some cases logarithmically) to lake surface area and maximum depth. Therefore, surface water temperatures can be predicted with a knowledge of only air temperature, lake surface area, and maximum depth.

References

ANDERSON, N. J., AND O. BENNIKE. 1997. Holocene lake sediments in West Greenland and their paleoclimatic and paleoecological implications. Geol. Greenland Surv. Bull. **176:** 89–94.

———, AND K. P. BRODERSEN. 2001. Determining the date of ice-melt for low Arctic lakes along Søndre Strømford, southern West Greenland. Geol. Greenland Surv. Bull. **189:** 54–58.

———, R. HARRIMAN, D. B. RYVES, AND S. T. PATRICK. 2001. Dominant factors controlling variability in the ionic composition of West Greenland Lakes. Arct. Antarct. Alp. Res. **33:** 418–425.

ARAI, T. 1981. Climatic and geographic influences on lake temperature. Verh. Int. Limnol. **21:** 130–134.

BILELLO, M. A. 1964. Method for predicting river and lake ice formation. J. Appl. Meteorol. **3:** 38–44.

BROCK, T. D. 1981. Calculating solar radiation for ecological studies. Ecol. Model. **14:** 1–19.

BRODERSEN, K. P., AND N. J. ANDERSON. 2002. Distribution of chironomids (Diptera) in low arctic West Greenland lakes: Trophic conditions, temperature and environmental reconstruction. Freshw. Biol. **47:** 1137–1157.

CATALAN, J. 1988. Physical properties of the environment relevant to the pelagic ecosystem of a deep high-mountain lake (Estany Redó, Central Pyrenees). Oecol. Aquat. **9:** 89–123.

COOPER, P. I. 1969. The absorption of solar radiation in solar stills. Sol. Energy **12:** 333–346.

DINGMAN, S. L. 1972. Equilibrium temperatures of water surface as related to air temperature and solar radiation. Water Resour. Res. **8:** 42–49.

EDINGER, J. E., D. W. DUTTWEILER, AND J. C. GEYER. 1968. The response of water temperatures to meteorological conditions. Water Resour. Res. **4:** 1137–1144.

FANG, X., AND H. G. STEFAN. 1996. Long-term lake water temperature and ice cover simulations/measurements. Cold Reg. Sci. Technol. **24:** 289–304.

FEE, E. J., R. E. HECKY, S. E. M. KASIAN, AND D. R. CRUIKSHANK. 1996. Effects of lake size, water clarity, and climatic variability on mixing depths in Canadian shield lakes. Limnol. Oceanogr. **41:** 912–920.

HANN, B. J., B. G. WARNER, AND W. F. WARWICK. 1992. Aquatic invertebrates and climate change: A comment on Walker et al. (1991). Can. J. Fish. Aquat. Sci. **49:** 1274–1276.

HANNA, E., AND J. CAPPELEN. 2003. Recent cooling in coastal southern Greenland and relation with the North Atlantic Oscillation. Geophys. Res. Lett. (article 1132) **30**(3).

———, AND P. VALDES. 2001. Validation of ECMWF (re) analysis surface climate data, 1979–1998, for Greenland and implications for mass balance modelling of the ice sheet. Int. J. Climatol. **21:** 171–195.

HONDZO, M., AND H. G. STEFAN. 1993. Lake water temperature simulation model. J. Hydraul. Eng. ASCE **119:** 1251–1273.

HOTTEL, H. C. 1976. A simple model for estimating the transmittance of direct solar radiation through clear atmosphere. Sol. Energy **18:** 129–134.

KASTEN, F., AND G. CZEPLAK. 1980. Solar and terrestrial radiation dependent on the amount and type of cloud. Sol. Energy **24:** 177–189.

KRAUS, E., AND J. TURNER. 1967. A one-dimensional model of the seasonal thermocline. II. The general theory and its consequences. Tellus **19:** 98–105.

LIU, B. Y. H., AND R. C. JORDAN. 1960. The interrelationship and characteristic distribution of direct, diffuse and total solar radiation. Sol. Energy **4:** 1–19.

LIVINGSTONE, D. M., AND A. F. LOTTER. 1998. The relationship between air and water temperatures in lakes of the Swiss Plateau: A case study with palaeolimnological implications. J. Paleolimnol. **19:** 181–198.

———, ———, AND I. R. WALKER. 1999. The decrease in summer water temperature with altitude in Swiss alpine lakes: A comparison with air temperature lapse rates. Arct. Antarct. Alp. Res. **31:** 341–352.

LORENZ, E. N. 1956. Empirical orthogonal functions and statistical weather prediction. Statistical Forecasting Scientific Rep. 1, Department of Meteorology, Massachusetts Institute of Technology.

LOTTER, A. F., H. J. B. BIRKS, W. HOFMANN, AND A. MARCHETTO. 1997. Modern diatom, cladocera, choronomid, and chrysophyte cyst assemblages as quantititative indicators for the reconstruction of past environmental conditions in the Alps. I. Clim. J. Paleolimnol. **18:** 395–420.

MCCOMBIE, A. M. 1959. Some relations between air temperatures and the surface water temperatures of lakes. Limnol. Oceanogr. **4:** 252–258.

MCGOWAN, S., D. B. RYVES, AND N. J. ANDERSON. 2003. Holocene records of effective precipitation in West Greenland. Holocene **13:** 239–249.

PEETERS, F., D. M. LIVINGSTONE, G. H. GOUDSMIT, R. KIPFER, AND R. FORSTER. 2002. Modeling 50 yr of historical temperature profiles in a large Central European lake. Limnol. Oceanogr. **47:** 186–197.

RODHE, B. 1952. On the relation between air temperature and ice formation in the Baltic. Geografisca Annaler. **34:** 175–202.

SHUTER, B. J., D. A. SCHLESINGER, AND A. P. ZIMMERMAN. 1983. Empirical predictors of annual surface water temperature cycles in North American lakes. Can. J. Fish. Aquat. Sci. **40:** 1838–1845.

STEFAN, H. G., X. FANG, AND M. HONDZO. 1998. Simulated climate change effects on year-round water temperatures in temperate zone lakes. Clim. Change **40:** 547–576.

STRASKRABA, M. 1980. The effects of physical variables on freshwater production: Analyses based on models, p. 13–84. *In* E. D. LeCren [ed.], The functioning of freshwater ecosystems. Cambridge Univ. Press.

SWEERS, H. E. 1976. A nomogram to estimate the heat-exchange coefficient at the air–water interface as a function of wind speed and temperature; a critical survey of some literature. J. Hydrol. **30:** 375–401.

THOMPSON, S. L., AND D. POLLARD. 1997. Greenland and Antarctic mass balances for present and doubled atmospheric CO2 from the GENESIS version 2 global climate model. J. Clim. **10:** 871–900.

WILLIAMS, W. D. 1991. Comments on the so-called salt lakes of Greenland. Hydrobiologia **210:** 67–74.

Received: 12 December 2002
Accepted: 4 August 2003
Amended: 11 September 2003